Aspect Ratios of Natural Ice Crystals in Ice Clouds

Junshik Um and Greg M. McFarquhar, University of Illinois, junum@illinois.edu

1. INTRODUCTION

- Ice clouds consist of non-spherical ice crystals with various shapes (i.e., habits) and sizes
- Accurate length (*L*) – width (*W*) relationships are important for determining single-scattering and physical properties (e.g., fall velocities) of ice crystals
- Past *L-W* relationships derived from limited number of crystals observed over limited temperature and humidity ranges
- *L* and *W* of columns and plates and individual branches of bullet rosettes obtained from high-resolution ice crystal images recorded by a Cloud Particle Imager during 2006 Tropical Warm Pool International Cloud Experiment (TWP-ICE) in Tropics, 2008 Indirect and Semi-Direct Aerosol Campaign (ISDAC) in Arctic, and 2010 Small Particles in Cirrus (SPARTICUS) campaign in mid-latitudes

2. METHODOLOGY & DATA

- Ice crystals classified using Um and McFarquhar (2009) scheme; only well-defined columns, plates, & bullet rosettes used in subsequent analysis so that dimensions unambiguously measured
- New software, "Ice Crystal Ruler (IC-Ruler)", developed at University of Illinois, determines maximum dimension (*D*), length (*L*), and width (*W*) of columns, plates, bullets and horizontally-oriented columns (Fig. 1 and Tables 1, 2, 3)

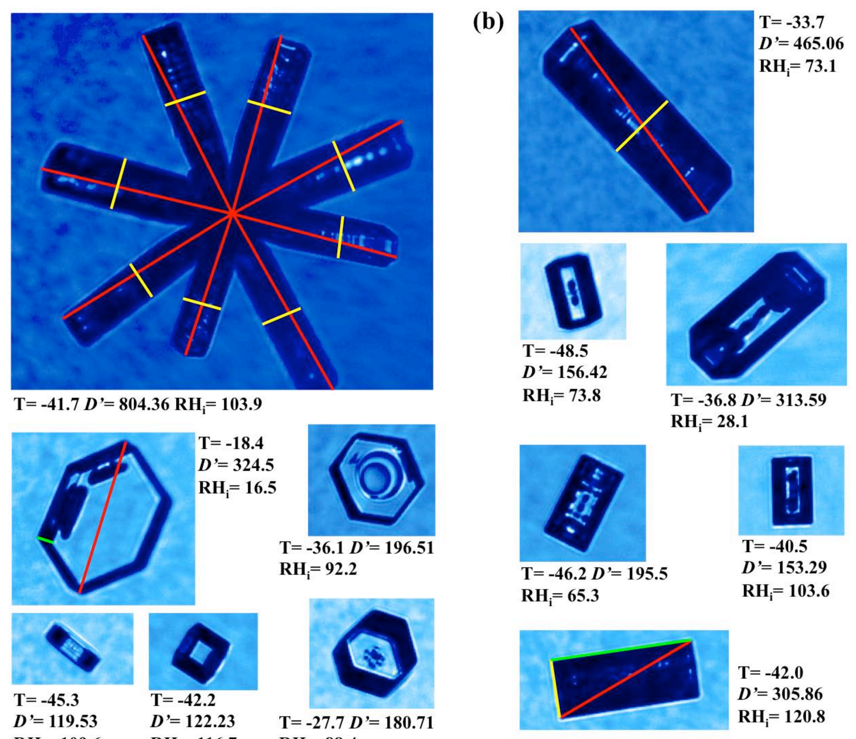

Fig.1. Example CPI images of (a) bullet rosette, (b) columns, and (c) plates during SPARTICUS. Projected maximum dimension (*D'*, red), width (*W'*, yellow), and length (*L'*, green) indicated for first crystal in each panel. Temperature (T, °C), *D'* (μm), and relative humidity with respect to ice (RH_i, %) also indicated. For columns upper three images are columns with orientations, whereas lower three are horizontally oriented with respect to imaging plane.

Table 1. # of crystals of each habit analyzed from SPARTICUS, together with range of temperature and humidity. Total # of bullet rosettes and # of bullets, as well as mean and standard deviation of # of branches per rosette also shown in bullet rosette column.

Flight Date	T (°C)	RHi (%)	Number of samples		
			Column (HCOL)	Plate	Bullet rosette (# of branch)
0119A	-56.0 − -18.8	17.8 − 123.3	619 (168)	38	199 (1071, 5.4±1.1)
0120A	-59.3 − -43.3	42.4 − 148.4	648 (166)	48	592 (3489, 5.9±1.2)
0120B	-58.1 − -11.6	9.2 − 63.5	436 (96)	30	318 (1817, 5.7±1.3)
0211B	-47.8 − -31.5	85.1 − 127.6	214 (45)	14	576 (3495, 6.1±1.3)
0323A	-60.4 − -12.4	53.6 − 181.7	133 (39)	10	51 (314, 6.2±1.1)
0330A	-60.2 − -26.8	47.8 − 141.8	120 (38)	14	105 (696, 6.6±1.1)
0330B	-58.5 − -29.9	63.6 − 141.1	235 (56)	25	236 (1206, 5.1±1.1)
0401A	-54.2 − -38.0	19.9 − 199.7	374 (92)	6	482 (2825, 5.9±1.3)
0401B	-51.6 − -21.7	58.6 − 139.3	164 (31)	31	216 (1387, 6.4±1.4)
0402A	-59.3 − -18.6	65.9 − 146.8	209 (60)	11	41 (271, 6.6±1.0)
0428A	-66.9 − -50.7	8.1 − 117.1	180 (65)	3	4 (22, 5.5±1.0)
0428B	-65.8 − -31.3	12.9 − 137.8	295 (86)	12	104 (595, 5.7±1.2)
0429	-64.5 − -9.6	16.1 − 141.5	88 (21)	5	106 (719, 6.8±1.1)
0614	-52.3 − -20.0	80.5 − 154.0	138 (57)	185	12 (64, 5.3±1.1)
0615A	-51.1 − -19.7	56.8 − 123.4	54 (8)	215	5 (21, 4.2±0.8)
0624A	-50.6 − -28.9	81.9 − 145.4	138 (24)	15	78 (503, 6.4±1.2)
Total			4045 (1052)	662	3125 (18495, 5.9±1.3)

Table 2. Same as Table 1, but for TWP-ICE. NA denotes that corresponding data not available.

Flight Date	T (°C)	RHi (%)	Number of samples		
			Column (HCOL)	Plate	Bullet rosette (# of branch)
0125	-70.2 − -51.4	NA	294 (80)	20	74 (432, 5.8±1.1)
0127	-81.5 − -45.5	NA	289 (64)	63	84 (551, 6.6±1.3)
0129	-74.5 − -37.7	NA	299 (54)	15	372 (2488, 6.7±1.3)
0202	-67.8 − -18.3	NA	282 (75)	143	90 (559, 6.2±1.3)
0206	-73.1 − -40.2	NA	271 (78)	439	0
0210	-78.7 − -40.5	NA	394 (46)	1049	0
0212	-72.7 − -34.1	NA	148 (33)	359	131 (720, 5.5±1.2)
Total			1977 (430)	2088	751 (4750, 6.3±1.3)

Table 3. Same as Table 2, but for ISDAC

Flight Date	T (°C)	RHi (%)	Number of samples		
			Column (HCOL)	Plate	Bullet rosette (# of branch)
0404	-39.4 − -1.0	68.7 − 133.2	745 (272)	84	45 (260, 5.8±1.0)
0405	-38.3 − -14.0	69.2 − 135.1	325 (91)	50	21 (116, 5.5±0.8)
0413	-33.7 − -16.4	87.8 − 115.4	72 (13)	9	37 (227, 6.1±1.5)
0419	-33.5 − -8.5	53.8 − 110.8	409 (121)	19	304 (1455, 4.8±1.0)
0425	-36.0 − -4.0	67.8 − 137.5	634 (175)	126	279 (1361, 4.9±0.8)
0427	-36.3 − -16.5	37.6 − 133.0	493 (155)	60	75 (351, 4.7±0.9)
Total			2678 (827)	348	761 (3770, 5.0±1.0)

3. RESULTS

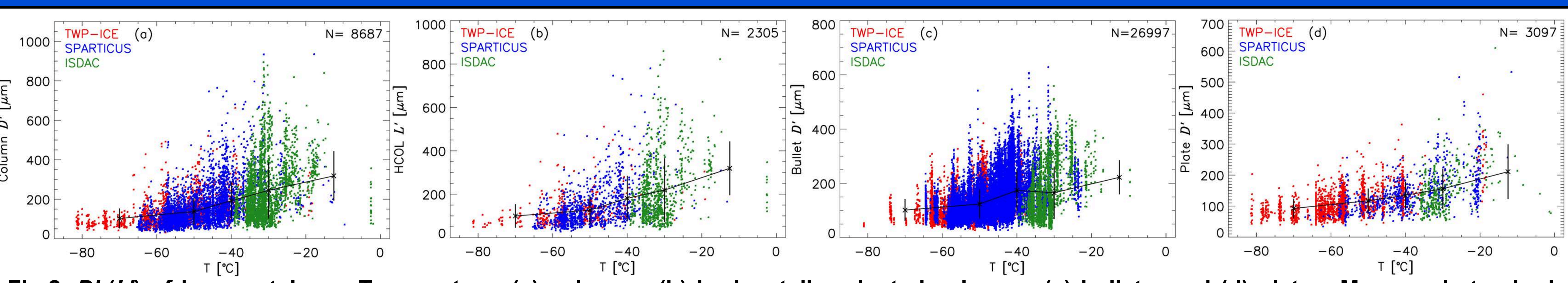

Fig.2. *D'* (*L'*) of ice crystals vs. Temperature. (a) columns, (b) horizontally oriented columns, (c) bullets, and (d) plates. Mean and standard deviations also shown.

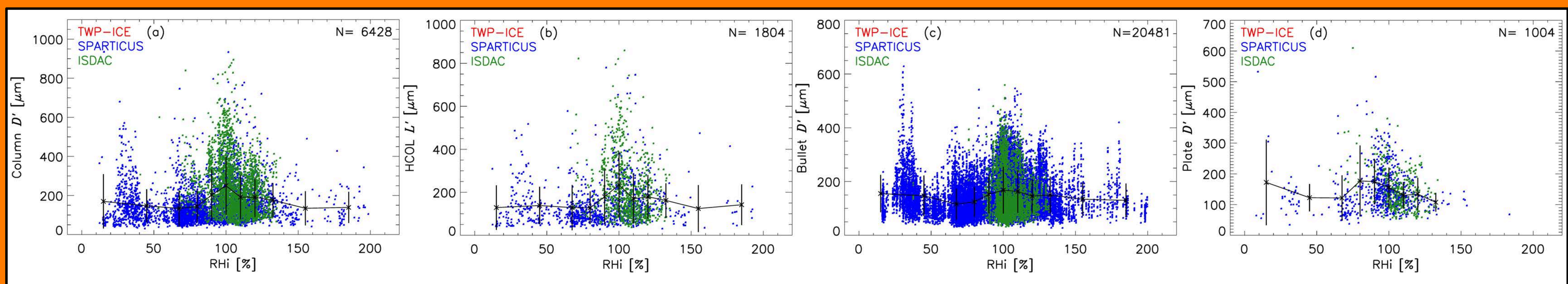

Fig.3. Same as Fig. 2, but as function of RH_i.

- Statistical distribution of *D'* (*L'*) of ice crystals strongly depends on T (Fig. 2).
- Largest dimensions of ice crystals shown at ~ 100 % RH_i (Fig. 3).

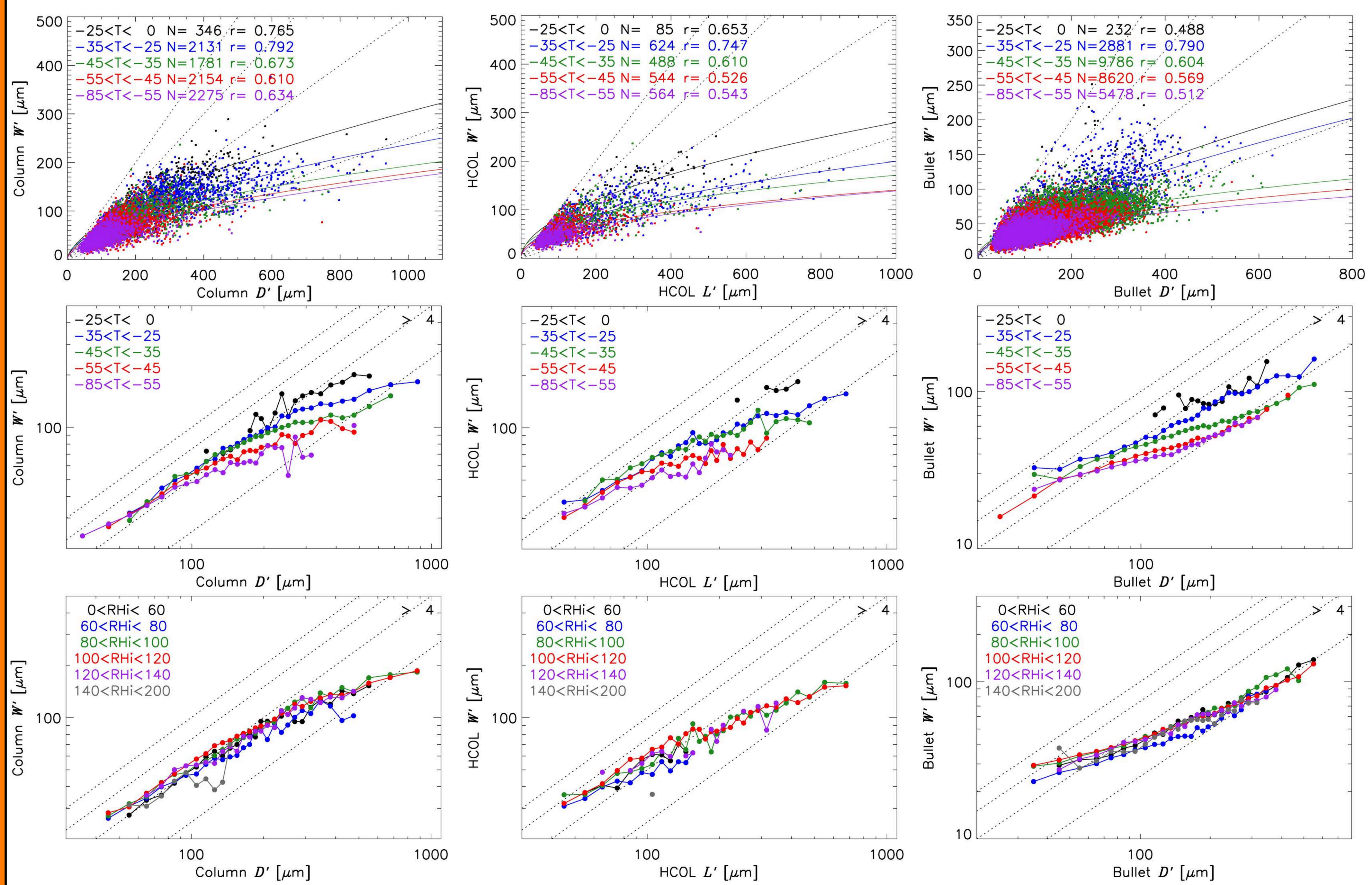

Fig.4. *W'* as function of *D'* or *L'* for columns (left column), horizontally oriented columns (middle column), and bullets (right column) as a function of T (top row). Mean width for given size ranges of *D'* or *L'* shown as functions of T (middle row) and RH_i (bottom row). Aspect ratios of 1.0, 0.75, 0.5, and 0.25 are indicated with dashed lines in each panel.

- Relationship between *L'* (*D'*) with *W'* showed T dependence (top row in Fig. 4).
- For given *L'* or *D'*, *W'* increased with T (middle row in Fig. 4), whereas there was no clear dependence on RH_i (bottom row in Fig. 4).

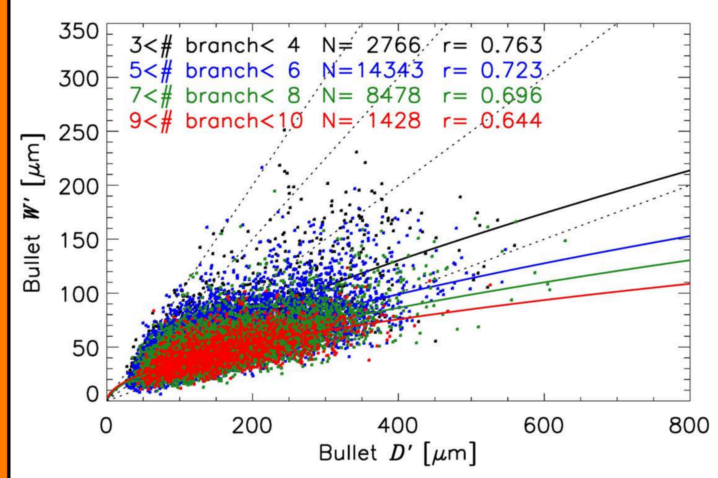

Fig.5. Bullet *D'* vs. *W'* as a function of # of bullet branches.

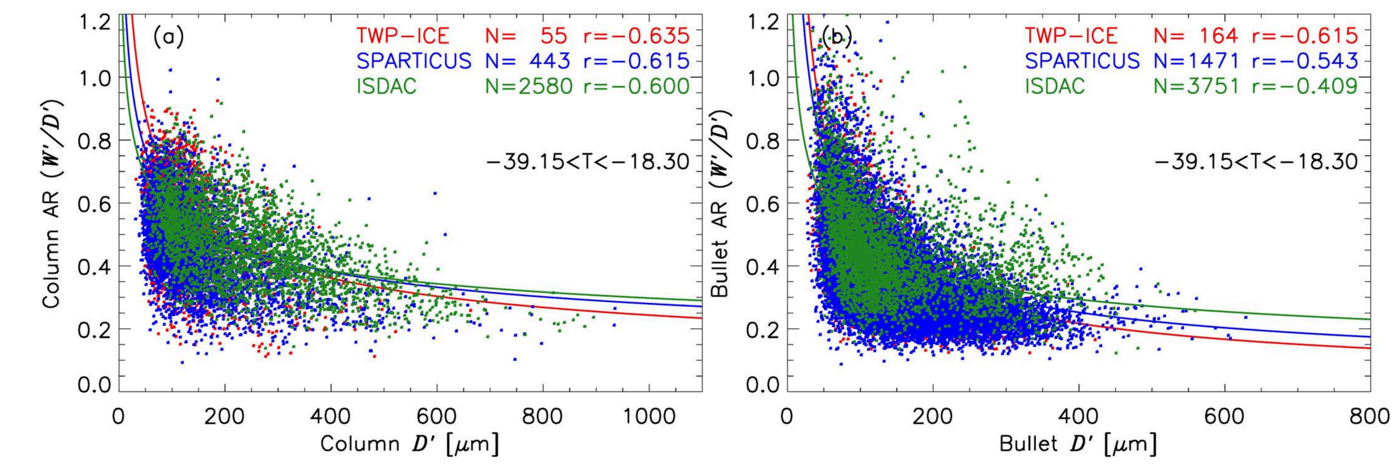

Fig.6. Aspect ratios vs. *D'* of (a) columns and (b) bullets at -39.15 < T < -18.30 °C at which all three campaigns made measurements.

- Aspect ratios of bullets increase as # of branches in bullet rosettes decrease (Fig. 5).
- No clear dependence of aspect ratio on the geophysical location (Fig. 6).

4. SUMMARY & FUTURE WORK

- Large data base on dimensions of ice crystals has been built.
- All measured dimensions of ice crystals increase with T (Fig. 2).
- Weak dependence of dimensions on RH_i shown, with largest dimensions found at ~100% RH_i (Fig. 3).
- Relationships between *L'* (*D'*) and *W'*, (i.e., aspect ratios) depend heavily on T, but not RH_i (Fig. 4).
- For given *L'* or *D'*, *W'* increased with T (Fig. 4).
- For given *D'*, aspect ratios (*W'*/*D'*) of bullets increase with decrease of # of branches (Fig. 5).
- No clear dependence of aspect ratio on geophysical location, but further analysis is required (Fig. 6).
- An iterative approach (Um and McFarquhar 2007) will be applied to take into account impacts of particle orientations on measured dimensions.

REFERENCES & ACKNOWLEDGEMENTS

Um, J., and G. M. McFarquhar, 2007: Single-scattering properties of aggregates of bullet rosettes in cirrus cloud. *J. Appl. Meteor. Climatol.*, 46, 757-775, doi:10.1175/JAM250.1.

Um, J., and G. M. McFarquhar, 2009: Single-scattering properties of aggregates of plates. *Quart. J. Roy. Meteor. Soc.*, 135, 291-304, doi: 10.1002/qj.378.

This research was supported by DOE under grant number DE-FG02-09ER64770, DE-SC0001279, and DE-SC0008500. Data were obtained from the ARM program archive.